Supporting Information

Excited-State Dynamics of [Ru(S–Sbpy)(bpy)2]2+ to Form Long-Lived Localized Triplet States

Moritz Heindl,[1] Jiang, Hongyan,[2] Shao-An Hua,[3] Manuel Oelschlegel,[3] Franc Meyer,[3] Dirk Schwarzer,[2] Leticia González[1,4]

1Institute of Theoretical Chemistry, Faculty of Chemistry, University of Vienna, A-1090 Vienna, Austria

2 Department of Dynamics at Surfaces, Max-Planck-Institute for Biophysical Chemistry, D-37077 Göttingen, Germany

3 Institute of Inorganic Chemistry, University of Göttingen, D-37077 Göttingen, Germany

4 Vienna Research Platform on Accelerating Photoreaction Discovery, University of Vienna, A-1090 Vienna, Austria

Table of contents

S1. Geometry optimization

All optimizations have been conducted at the B3LYP/6-311G(d)-LANL2DZ level of theory employing all the additional parameters stated in the Computational details section of the main manuscript except for Douglas-Kroll-Hess integrals. A sample input for g09 is given below (note that this is not the optimized geometry!), followed by the Cartesian Coordinates of the optimized S_0 and T_1 geometries.

#p opt B3LYP/Genecp EmpiricalDispersion=GD3 SCRF(PCM,Solvent=Acetonitrile) nosymm pop=full

ru(bpy) s-bridged excited states, guess geometry

+2 3

Ru	0.524363	0.046544	-0.009953
N	-1.080882	-0.831526	-1.042256
N	-1.109235	0.589360	1.193178
N	1.987430	1.152914	1.011532
N	0.404037	1.915819	-0.970669
N	2.066846	-0.754069	-1.189343
N	0.881170	-1.800421	0.937122

C	-0.968320	-1.466759	-2.223058
C	-2.313422	-0.589871	-0.514353
C	-2.312808	0.085935	0.800435
C	-1.005890	1.249161	2.361348
C	2.763733	0.679179	2.004532
C	2.155180	2.438480	0.590020
C	1.257916	2.870151	-0.501407
C	-0.452258	2.231403	-1.960573
C	2.529179	-1.977088	-0.803303
C	2.629272	-0.142039	-2.248894
C	0.213597	-2.270844	2.007559
C	1.851568	-2.570975	0.367541
C	-2.077805	-1.872248	-2.956983
C	-3.477103	-0.930484	-1.236828
C	-3.435765	0.179804	1.650246
C	-2.089271	1.419945	3.216352
C	3.736538	1.451556	2.629928
C	3.119236	3.263054	1.178736
C	1.254424	4.160593	-1.040227
C	-0.501896	3.496290	-2.536567
C	3.575023	-2.596333	-1.495310
C	3.669308	-0.708824	-2.977526
C	0.473853	-3.517149	2.567182
C	2.156752	-3.834132	0.884106
C	-3.349044	-1.589045	-2.464914
S	-5.092769	-0.368482	-0.734522
S	-4.937883	-0.723010	1.323352
C	-3.317250	0.866559	2.863735
C	3.917563	2.769034	2.207672
C	0.369050	4.479623	-2.066971
C	4.151575	-1.959945	-2.591878
C	1.464618	-4.314040	1.993433
H	-4.236124	-1.872034	-3.023029
H	-1.944846	-2.389791	-3.900891
H	0.040941	-1.630769	-2.580406
H	-4.177607	0.961424	3.518919
H	-1.966978	1.966248	4.145368
H	-0.021216	1.626841	2.608045
H	2.584426	-0.349171	2.295684
H	4.335424	1.024297	3.426818
H	4.667666	3.402815	2.669559
H	3.251538	4.283316	0.839772
H	1.932769	4.915952	-0.662580
H	0.359189	5.479170	-2.489419
H	-1.210300	3.699651	-3.332186
H	-1.109838	1.436607	-2.291569

H	-0.547571	-1.618152	2.418079
H	-0.092100	-3.850162	3.430318
H	1.694850	-5.293730	2.399463
H	2.925165	-4.444526	0.425617
H	3.942607	-3.566616	-1.184134
H	4.963715	-2.433697	-3.133803
H	4.088052	-0.176447	-3.824574
H	2.220111	0.827490	-2.507977

C H N S 0
6-311G(d)
****
Ru 0
LANL2DZ
****

Ru 0
LANL2DZ

S2.1 Optimized S_0 geometry

Ru	0.521442	0.024655	-0.007272
N	-1.083240	-0.829668	-1.037170
N	-1.108290	0.584119	1.196080
N	1.981500	1.145710	1.014190
N	0.403755	1.908620	-0.966056
N	2.057620	-0.752925	-1.191830
N	0.886759	-1.801680	0.935176
C	-0.970719	-1.468470	-2.212480
C	-2.312910	-0.583533	-0.512371
C	-2.311000	0.087831	0.801960
C	-1.004670	1.246370	2.359270
C	2.751860	0.671691	2.007260
C	2.146570	2.429900	0.597506
C	1.257790	2.859270	-0.498894
C	-0.443555	2.219530	-1.960730
C	2.524030	-1.972020	-0.809543
C	2.610580	-0.138683	-2.250890
C	0.230510	-2.269110	2.009680
C	1.853850	-2.567790	0.361729
C	-2.077300	-1.871030	-2.944400
C	-3.470510	-0.920737	-1.237040
C	-3.429610	0.190633	1.648770

C	-2.086560	1.425710	3.207400
C	3.714910	1.445470	2.637840
C	3.098800	3.255990	1.194190
C	1.265630	4.142370	-1.045570
C	-0.482299	3.477800	-2.542980
C	3.566680	-2.585940	-1.503280
C	3.647770	-0.700697	-2.980290
C	0.497999	-3.511010	2.566390
C	2.165160	-3.826540	0.875219
C	-3.345420	-1.579550	-2.459370
S	-5.086730	-0.347112	-0.742254
S	-4.934110	-0.713782	1.325680
C	-3.313240	0.877434	2.856390
C	3.890450	2.762080	2.223430
C	0.389722	4.456530	-2.076940
C	4.134970	-1.946590	-2.597800
C	1.482900	-4.304440	1.986910
H	-4.229490	-1.854620	-3.021690
H	-1.942510	-2.389120	-3.885100
H	0.035024	-1.635470	-2.571100
H	-4.170460	0.974719	3.511540
H	-1.961380	1.972100	4.133300
H	-0.021796	1.618580	2.611240
H	2.576420	-0.354876	2.298150
H	4.308900	1.016970	3.434880
H	4.632080	3.397320	2.692310
H	3.225680	4.277120	0.862719
H	1.947100	4.894510	-0.673256
H	0.389343	5.450760	-2.506970
H	-1.183650	3.676200	-3.343280
H	-1.101160	1.428970	-2.294260
H	-0.524370	-1.619390	2.430040
H	-0.059817	-3.840450	3.433550
H	1.718070	-5.281330	2.391650
H	2.930930	-4.433920	0.413316
H	3.938380	-3.553380	-1.195330
H	4.946000	-2.415990	-3.141260
H	4.059190	-0.165701	-3.826580
H	2.196910	0.825614	-2.512240

S2.2 Optimized T_1 geometry

Ru	0.489551	0.036322	-0.010251
N	-1.120930	-0.817924	-1.017390

N	-1.139690	0.563483	1.175720
N	1.973470	1.126470	1.001770
N	0.372842	1.911380	-0.953134
N	2.047500	-0.742978	-1.186650
N	0.854903	-1.814570	0.918265
C	-0.947937	-1.474790	-2.164400
C	-2.377800	-0.588621	-0.505905
C	-2.374040	0.084227	0.800803
C	-0.977145	1.253920	2.304190
C	2.755340	0.641516	1.980470
C	2.143110	2.410810	0.587895
C	1.240630	2.852900	-0.492451
C	-0.487713	2.235650	-1.932140
C	2.526420	-1.954930	-0.797430
C	2.609020	-0.119149	-2.235600
C	0.181520	-2.299000	1.974540
C	1.843810	-2.563960	0.359931
C	-2.012750	-1.929560	-2.938530
C	-3.508580	-0.954730	-1.298330
C	-3.462480	0.228118	1.714890
C	-2.020640	1.497590	3.193910
C	3.735300	1.403930	2.598680
C	3.111960	3.226130	1.172720
C	1.249720	4.139520	-1.031060
C	-0.526116	3.497950	-2.505380
C	3.591060	-2.551370	-1.472900
C	3.667930	-0.663532	-2.946940
C	0.455109	-3.540250	2.529490
C	2.163440	-3.820660	0.873659
C	-3.287240	-1.644960	-2.515450
S	-5.172820	-0.592766	-0.982445
S	-5.045960	-0.461453	1.578630
C	-3.251980	0.962535	2.907850
C	3.915690	2.720740	2.186880
C	0.360545	4.467020	-2.046690
C	4.168450	-1.901670	-2.556460
C	1.465150	-4.314910	1.967970
H	-4.142580	-1.944340	-3.108150
H	-1.825250	-2.466740	-3.859080
H	0.074147	-1.623450	-2.481600
H	-4.080740	1.093920	3.592280
H	-1.844560	2.071450	4.094330
H	0.023119	1.606770	2.509600
H	2.575000	-0.384488	2.270640
H	4.338030	0.967050	3.384520
H	4.670200	3.347510	2.646510

H	3.242410	4.247650	0.843969
H	1.942410	4.884240	-0.664569
H	0.361091	5.464010	-2.470260
H	-1.238590	3.706990	-3.293040
H	-1.156660	1.452510	-2.260580
H	-0.593054	-1.663890	2.381070
H	-0.117221	-3.883720	3.381610
H	1.706660	-5.290250	2.372720
H	2.947930	-4.413790	0.424870
H	3.972980	-3.512940	-1.159130
H	4.996610	-2.357330	-3.085590
H	4.085520	-0.121362	-3.785600
H	2.184400	0.838605	-2.503720

S2. Classification Scheme

The flow of electronic charge for all considered excited states of $[Ru(^{S\text{-}S}bpy)(bpy)_2]^{2+}$ is discussed in terms of charge transfer. Depending on the localization of the hole (from where the electron is excited) and the excited electron, a total of ten different types of excitations can be discerned with the four fragments (M, S, L, and L) employed. In three of those, the electron is located at the same fragment as the hole: MC, SC, and LC. The other seven represent contributions of charge transfer processes: SMCT, LMCT, MSCT, LSCT, MLCT, SLCT, and LLCT, where the first letter always denotes the hole fragment and the second denotes the electron fragment. All possible excitations are depicted in **Figure S1Error! Reference source not found.**.

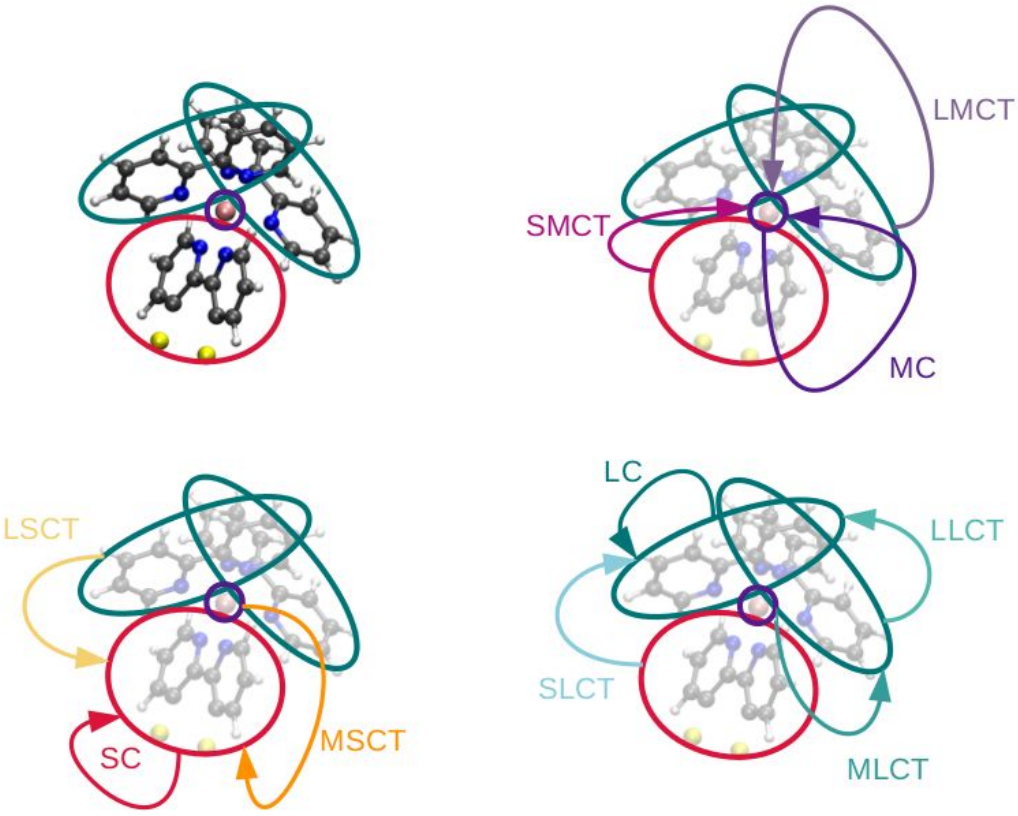

Figure S1. Structure of $[Ru^{S\text{-}S}bpy(bpy)_3]^{2+}$ and the segmentation into the 4 fragments used in this work. All resulting transitions, their labels and their corresponding colors are also shown.

S3. LVC template modifications

S3.1 Mode reduction

Using the complete set of 177 vibrational modes in the LVC template and optimizing the T_1 state results in geometries and energy gaps to the lowest singlet state that are not in line with the TD-DFT optimization. While structural changes that define the TD-DFT T_1 minimum energy structure, namely the elongation of the S-S bond at the $^{S\text{-}S}$bpy, are observed within the LVC optimization, the extent of this elongation and the obtained energy gap are underestimated. In an attempt to systematically search for modes that are badly described in the employed LVC model and to

enhance the applicability of the LVC Hamiltonian, a search for modes that result in a mismatch between the TD-DFT and the LVC T_1 geometries and energies has been conducted of which the main results are presented in the main body of the text. A more detailed view on the divergence between the TD-DFT and LVC description of the T_1 state is presented here with special emphasis on the energy gap between the T_1 and the S_0 at the minimum energy T_1 geometry, as opposed to just the T_1 energy depicted in Figure 4. In **Figure S2**, a linear interpolation scan from the S_0 minimum energy geometry towards the T_1 minimum energy structure calculated with the respective model (either TD-DFT or an LVC model where the lowest 0 to 54 modes have been ignored) is shown. It is important to note, that the S_0 geometry for all the employed models is identical and only the T_1 geometry (and the path towards it) differs between different models. The black thick line represents the TD-DFT values that serve as the reference values. It can be seen that LVC Hamiltonians that employ all or almost all modes seem to result in T_1 minima that are far from the TD-DFT ones where both the T_1 and S_0 energies deviate by more than 1 eV each at the T_1 minimum energy geometry. This results in S_0 energies that are larger than the T_1 energy at the T_1 minimum energy geometry which is in stark contrast to the TD-DFT T_1-S_0 energy gap of 0.4 eV, with the T_1 energy being larger. When too many modes are removed, the S-S bond elongation is hampered as corresponding vibrational modes are taken out of the system, resulting in a smaller bond elongation and higher T_1 energies.

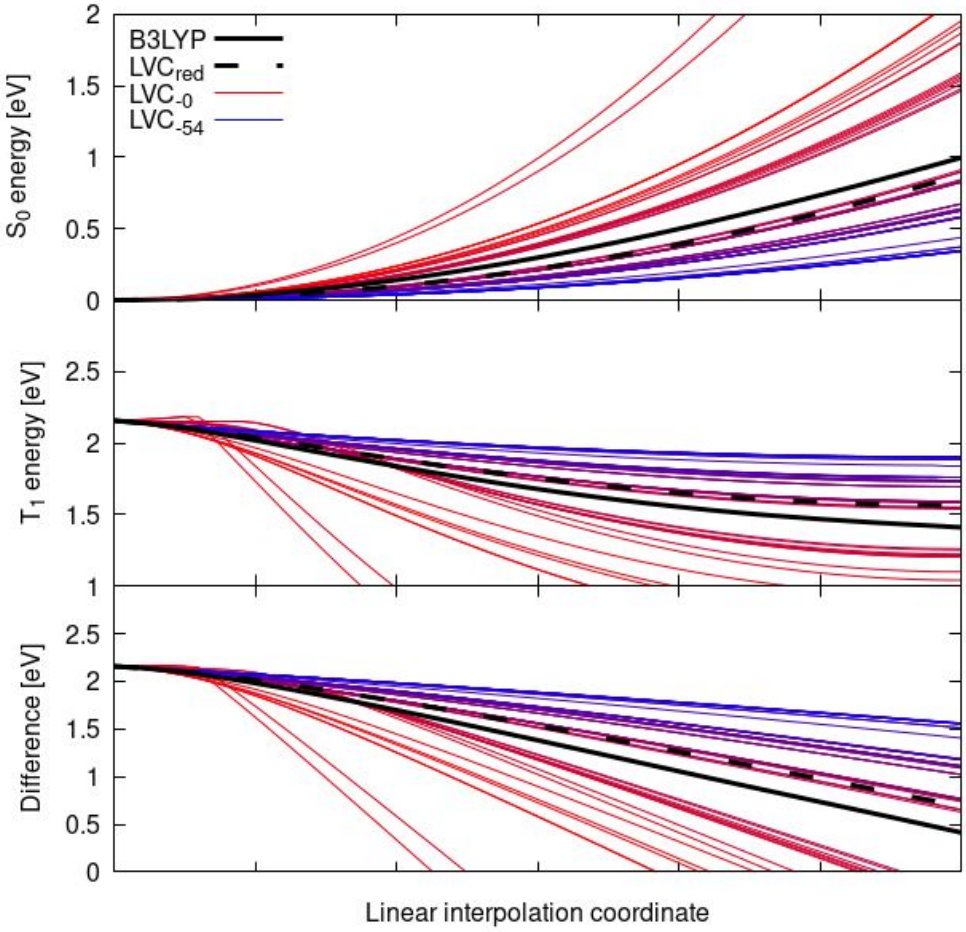

Figure S2. Linear interpolations between the FC geometry and the T_1 minimum energy geometry optimized at the respective level of theory. The black solid line represents the reference B3LYP values while the red to blue lines are scans resulting from using different LVC Hamiltonians that differ in the number of contained modes, starting from the complete set of modes (red) to a set of modes where 54 (blue) vibrational modes have been neglected. The top panel shows the energy of the lowest singlet state, the middle panel the respective T1 energy. The difference between the S_0 and the T_1 energies is plotted in the last panel.

The following modes (Table S1) have been removed from the complete parametrization as they were found to cause issues in the description of the T_1 state (see main text). The modes can also be visualized in the attached molden file.

ν_1	24 cm^{-1}	$^{S\text{-}S}$bpy flapping motion
ν_2	29 cm^{-1}	bpy flapping motions
ν_3	34 cm^{-1}	$^{S\text{-}S}$bpy-bpy twisting motion
ν_4	37 cm^{-1}	$^{S\text{-}S}$bpy-bpy twisting motion
ν_5	41 cm^{-1}	$^{S\text{-}S}$bpy-bpy twisting motion
ν_6	45 cm^{-1}	bpy wagging motion
ν_7	68 cm^{-1}	$^{S\text{-}S}$bpy wagging motion
ν_8	81 cm^{-1}	bpy bending motion
ν_9	85 cm^{-1}	bpy bending motion
ν_{10}	113 cm^{-1}	$^{S\text{-}S}$bpy bending motion
ν_{16}	181 cm^{-1}	$^{S\text{-}S}$bpy bending motion
ν_{17}	183 cm^{-1}	$^{S\text{-}S}$bpy twisting motion
ν_{20}	209 cm^{-1}	$^{S\text{-}S}$bpy twisting motion
ν_{23}	270 cm^{-1}	inter-bpy wagging motion
ν_{26}	303 cm^{-1}	$^{S\text{-}S}$bpy S-S asynchronous stretch
ν_{28}	328 cm^{-1}	Ru displacement motion

Table S1. Modes that have been removed to result in the LVC_{red} Hamiltonian that is used in the main manuscript.

S3.2 The T_{17} state

Initially, the full set of 21 singlet and 20 triplet states was used in the LVC_{red} template for dynamics simulations. When analyzing the final states of the dynamics simulations, two different triplet minima where accessible in the dynamics. One of those is the T_1 minimum energy structure presented in the main manuscript which features an elongated S-S bond on the $^{S\text{-}S}$bpy ligand. The other stable low-energy triplet state features a minimum at an energy gap between this and the lowest lying singlet state at this geometry of about 1 eV. This state will be termed T^* in the following. The LVC_{red} optimized T^* minimum energy geometry features two elongated Ru-bpy bonds and is of MLCT/LC character. When analyzing the T^* state in terms of diabatic reference states, a big contribution of the T_{17} (40%) state is found, which is the most prominent contribution. Participation of a Franck-Condon high-lying state in formation of another minimum structure with some considerable distance to the FC geometry is possible but in the case of such a simple LVC model, the validity of the LVC model to describe this minimum needs to be verified. To do so, it was tested if the same minimum energy geometry can be found in a TD-DFT optimization. For this a set of 10 geometries has been generated, that uses the T^* minimum energy geometry as a starting point with slightly elongated or shortened Ru-bpy bonds. This adaption of the initial geometries is done to take into account the possibility that there can be structural differences between the hypothetical TD-DFT/T^* and the already optimized LVC_{red}/T^* minimum energy structures. From every one of these points, an optimization in the lowest energy triplet state was conducted. It was found that all TD-DFT optimizations converged to the already presented T_1 minimum energy structure regardless of the initial starting geometry. Hence, this T* minimum was labelled an artifact that directly impacts the dynamics by presenting a competing low-energy

minimum structure that was accessed throughout the dynamics. For the main findings of this paper, the diabatic T_{17} state and all associated couplings have been removed from the Hamiltonian.

In the following, the influence of the presence of the T_{17} state on the dynamics is highlighted by showing the dynamics using a LVC_{red} template that still includes the T_{17} state (**Figure S3**). The initial evolution of the wave function during the first 75 fs is found to be independent of the inclusion of the diabatic T_{17} state and therefore identical to Figure 5 of the main manuscript. After 200 fs, the composition of the wavefunction stabilizes and only limited changes occur. Here, strong divergence from the dynamics without the diabatic T_{17} state are visible with a larger amount of population being located in MLCT and LC states when including the T_{17} state.

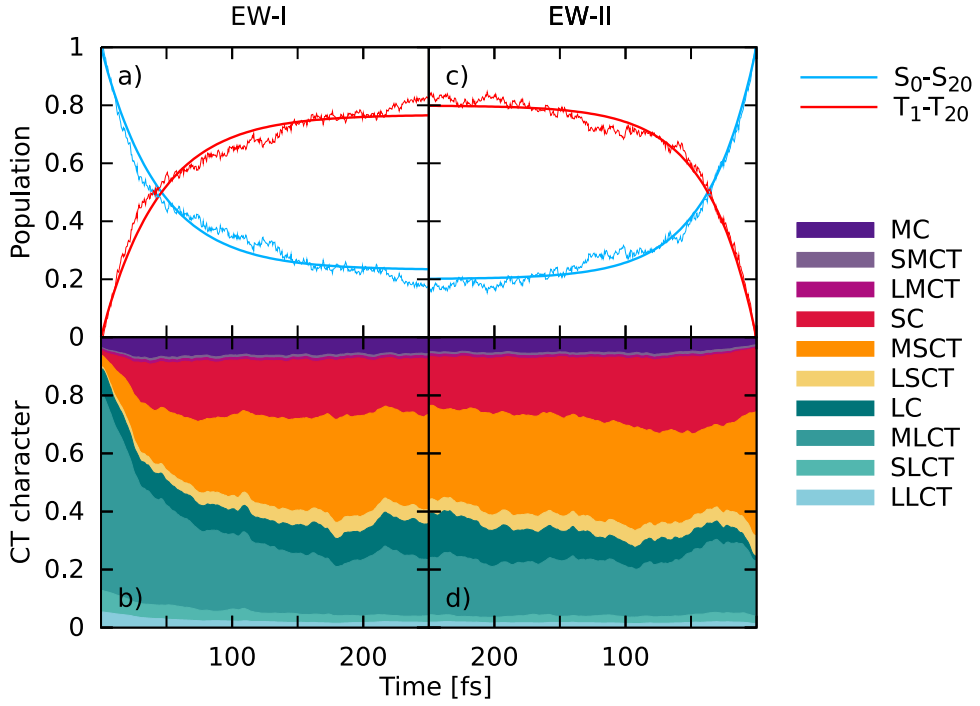

Figure S3. Excited state dynamics simulations of $[Ru(^{S-S}bpy)(bpy)_2]^{2+}$ for both excitation windows using the LVC_{red} Hamiltonian including the T_{17} state. Note the inverted time axis for the right hand side plots. a) and c): Sum of singlet and triplet populations for excitation in EW-I and

EW-II, respectively. Thin lines represent the sum of all trajectories and thick lines represent fits of the populations. b) and d): Evolution of charge transfer character.

S4. S-S bond length

The S-S bond length across the simulated dynamics is shown in Figure S4. The initial coherent movement of the bond length is clearly visible as is the trend to increase this bond length as more and more trajectories approach the T_1 minimum.

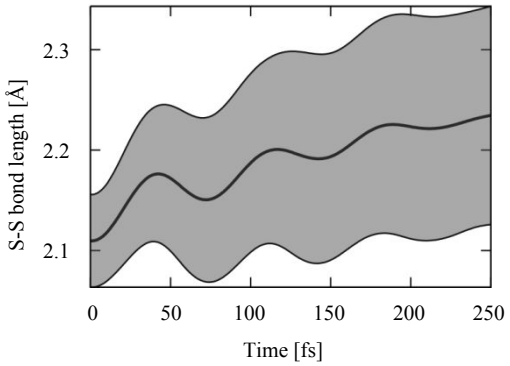

Figure S4. Change of the S-S bond length over the complete ensemble of trajectories. The gray represents the standard deviation at the corresponding time while the centered black line is the average of the S-S bond length.